Stresses in a Viscoelastic Fluid in Converging and Diverging Flow

E. B. ADAMS, J. C. WHITEHEAD, and D. C. BOGUE

University of Tennessee, Knoxville, Tennessee

Birefringent studies have been carried out on a viscoelastic fluid (polystyrene in Aroclor) flowing in straight, converging, and diverging channels, for the purpose of obtaining point-by-point stress data (the shear stress and the difference in normal stresses). A preliminary analysis in terms of the Coleman-Noll second order theory for viscoelastic fluids shows good agreement.

Constitutive equations for viscoelastic fluids are formulated in general tensor notation, good in multidimensional flows and in arbitrary coordinate systems. Because of the many complexities, however, experimental work has been primarily concerned with viscometric flows, such as flow in straight pipes, between parallel flat walls, between rotating concentric cylinders, etc. Out of this work have come several useful theories relating normal and shear stresses to shear rate. To fully test the theories, however, one must consider the problem of multidimensional flows, that is, those involving a change of cross section in the direction of flow. As a start on that problem, the present work has been concerned with the measurement of stresses in converging and diverging channels, using the birefringent method and a highly birefringent material, polystyrene in Aroclor. Eventually velocity data will also be obtained and other materials will be studied.

BIREFRINGENT THEORY

Birefringence as a hydrodynamic tool was quantitatively developed by Prados and Peebles (*21*) for a highly birefringent, inelastic material: Milling Yellow dye suspensions. The birefringent method is appealing for viscoelastic materials as well, since studies can be made without introducing probes into the system. The reliability of the technique depends, of course, on the reliability of the theory relating optical behavior to the stress and/or strain history.

In a general analysis of optical behavior one must have a relationship between the vector $\mathbf{D}_i$, the electric displacement or electric flux density, and the vector $\mathbf{E}_i$, the inducing electric field. This relationship is treated in the following form:

$$\mathbf{D}_i = \mathrm{K}_0\mathbf{E}_i + \mathbf{P}_i \qquad (1)$$

In a qualitative way $\mathbf{D}_i$ may be considered as the "effect" of the electric field (that is, the quantity whose rate of change is related to the curl of the magnetic field through Maxwell's field equations). It comprises two terms: the contribution of the electric field if no material were present ($\mathrm{K}_0\mathbf{E}_i$), and the contribution created by the action of the electric field on the material (the polarization $\mathbf{P}_i$).

For small polarizations $\mathbf{P}_i$ is assumed to be linearily related to the electric field through the equation

$$\mathbf{P}_i = \mathrm{K}_0\mathrm{X}^j{}_i\mathbf{E}^j \qquad (2)$$

The second-order tensor $\mathrm{X}^j{}_i$ is a dimensionless property of the material called the (dielectric) *susceptibility*. Basically, the theories are concerned with relating the susceptibility to the stress and/or strain history.

In theoretical continuum mechanics Coleman and Toupin (*8*) have presented a general treatment of dielectric effects in terms of a functional of the strain history. Introducing the concept of a memory functional (that is, the material "forgets" past strains with the passage of time), they carry through arguments for susceptibility as a function of strain history in a manner analogous to the simple fluid arguments for stress as a function of strain history. These functions are not, in general, related to each other, except that in the case of first-order (slow) flows the functions reduce to

$$\mathrm{X}^i_j = -\epsilon\,\delta^i_j + \xi\,d^i_j + \text{terms of higher order} \qquad (3)$$

$$\tau^i_j = -\mathrm{p}\,\delta^i_j + \eta\,d^i_j + \text{terms of higher order} \qquad (4)$$

Thus for first-order flows and for quantities evaluated in some plane 1-2 one can eliminate d^i_j to obtain

$$\mathrm{X}_{11} - \mathrm{X}_{22} = \text{const}\ (\tau_{11} - \tau_{22}) \qquad (5)$$

or, in the particular case of the principal values

$$\mathrm{X}_{\mathrm{I}} - \mathrm{X}_{\mathrm{II}} = \text{const}\ (\sigma_{\mathrm{I}} - \sigma_{\mathrm{II}}) \qquad (6)$$

J. C. Whitehead is with Tennessee Eastman Corporation, Kingsport, Tennessee.

Also, since the two tensors vary only by a constant, it follows that the location of the principal axes of susceptibility and stress will be identical (that is, $\chi_{opt} = \chi_{stress}$). Of interest is Coleman and Toupin's comment that the susceptibility tensor cannot be proved to be symmetric in general, although for a first-order theory such as Equation (3), it must be symmetric due to the symmetry of the deformation rate tensor.

The molecular theories date to the work of Kuhn and Grün (*11*), who developed a network model consisting of a chain of monomer links, each link with two anisotropic susceptibilities. The analysis is based on the assumption that in a simple extension the (statistically weighted) average extension of the polymer chains is the same as the extension of the macroscopic system. A parallel development for stress as a function of the stretching of the polymer chains is carried out. Treloar (*26*) extended the treatment to include general homogeneous strains (with principal extension ratios λ_I and λ_{II} in the I-II plane) to give as the final results

$$X_I - X_{II} = \text{const}\ (\lambda^2_I - \lambda^2_{II}) \tag{7}$$

$$\sigma_I - \sigma_{II} = \text{const}\ (\lambda_I{}^2 - \lambda^2_{II}) \tag{8}$$

The proportionality constants are functions of molecular properties and the absolute temperature. It is assumed throughout that the principal axes of stress, strain, and susceptibility coincide; thus $\chi_{opt} = \chi_{stress}$. Also from Equations (7) and (8) one has again Equation (6).

The analyses of Kuhn and Grün and of Treloar treat materials with definable reference states (rubbery solids). Lodge (*13*) has generalized the analysis to include materials whose present stress state is due to deformations occurring at many different times in the past (flowing polymer solutions). The form of his result is like that of Equations (7) and (8) except that, instead of having the principal extension ratios as the measure of the deformation, one has a molecular measure: a type of summed chain link displacements. As before, the deformation measure can be eliminated between Equations (7) and (8) to yield Equation (6). Lodge thus states that Equation (6) holds independently of how the stress state was achieved, although he points out that because the fluid analogs of Equations (7) and (8) are not related to measurable quantities, one has no check of the theory other than Equation (6). It is implicitly assumed that the principal axes of stress and susceptibility are the same; how either is related to the principal axes of the macroscopic deformation or deformation rate is not treated.

In actual practice one measures the difference in refractive indices $n_I - n_{II}$ in an experiment in which the light beam passes in the III direction. Nye (*17*) considered the problem of a sinusoidal plane electric field (a polarized light beam) passing through an optically anisotropic material. Applying Maxwell's field equations and assuming no magnetic susceptibility and no electrical conductivity, he showed that the velocities of light along the principal axes of susceptibility are given by

$$\frac{c}{v_I} \equiv n_I = \sqrt{1 + X_I} \tag{9}$$

and

$$\frac{c}{v_{II}} \equiv n_{II} = \sqrt{1 + X_{II}} \tag{10}$$

Authors dealing with molecular theories invoke the Lorentz-Lorenz equation to relate the averaged susceptibility to the refractive index (*11, 13, 26*). The details of this step are not presented, although the Lorentz-Lorenz equation is, in a general way, a second-order correction to Equation (1). The correction has to do with the disturbing effect of the polarization on the electric field itself. For principal refractive indices nearly equal to each other, it makes no significant difference in the final result [Equation (11)].

For principal refractive indices nearly equal to each other, one can combine Equations (6), (9), and (10) to obtain

$$n_I - n_{II} \approx C\ (\sigma_I - \sigma_{II}) \tag{11}$$

The constant C is called the *stress optical coefficient*. From the molecular theories one can deduce that it depends on the type of polymer, on the mean refractive index, and on temperature. It does not, however, depend on the concentration of the polymer, in the case of polymer solutions, except that the concentration must be high enough so that the birefringence of the solvent is negligible. Equation (11) together with Equation (12)

$$\chi_{opt} = \chi_{stress} \tag{12}$$

are the working equations in stress-birefringence studies.

In sum it can be said that these working equations are consistent with the continuum analysis of Coleman and Toupin in the range of slow (Newtonian) flow; nothing can be said more generally. It can also be said that Lodge's extension of the molecular theory rationalizes the use of these equations rather generally (in any homogeneous flow and independent of the constancy of the viscosity function). In the absence of an independent check, however, one would not wish to state that the molecular analysis has been verified in detail.

Equations (11) and (12) have been extensively used for polymeric materials by Philippoff and co-workers (*6, 18, 19*). Experimentally, the values of Δn and χ_{opt} can be obtained by straightforward optical methods, neglecting edge effects. The values of $\Delta\sigma$ and χ_{stress} have been obtained independently by mechanical means and in so doing it has been customary to make the "Weissenberg assumption," that the normal stresses in the two directions normal to the direction of flow are equal. Several investigators (*9, 14*) have shown that these stresses are not equal, although the difference between them is small and is probably negligible in many applications. Despite this difficulty Equations (11) and (12) have given good agreement over a wide range of concentrations and molecular weights for a variety of materials (*6, 18, 19*). Good evidence in support of them, apart from any independent measurement of $\Delta\sigma$, is that they permit one to rationalize the parameters Δn vs. $2\tau_{12}/\sin 2\ \chi_{opt}$ in plotting birefringence data. [The group $2\tau_{12}/\sin 2\ \chi_{stress}$ occurs naturally in stress analysis, as in Equation (13).] Such plots are linear even when the viscosity is strongly non-Newtonian.

It is assumed in the present work that Equations (11) and (12) can be extended unchanged into accelerative flows, these being a kind of time-dependent flow from the standpoint of the fluid elements. There is no explicit justification for this assumption, although there is some supporting evidence from dynamic studies. The linear molecular theory of Read (*23*) and linear dynamic data of Read (*24*), of Stein et al. (*25*), and of Yamada et al. (*29*), support the assumption that the stress optical coefficient is independent or nearly independent of frequency for polymers well above their glass transition temperatures. This statement does not apply to more solidlike materials, however. Thus the out-of-phase characteristics of stress and birefringence are a sensitive measure of crystallinity (*29*). But in sum the dynamic studies support the laws being used here for rubbery polymers at high temperatures (well above their glass transition temperatures) and for polymer solutions without entanglement complications (*18*, 1963).

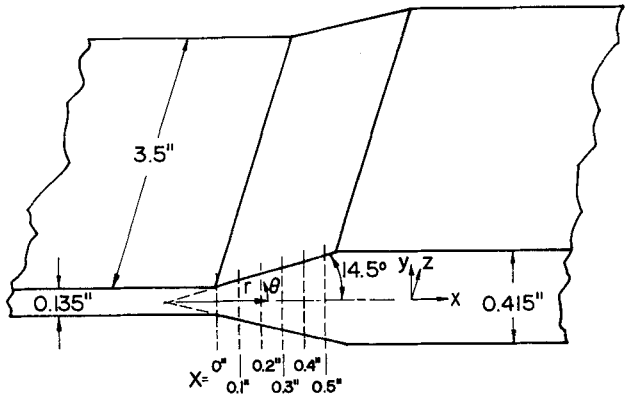

Fig. 1. Isometric view of the test channel.

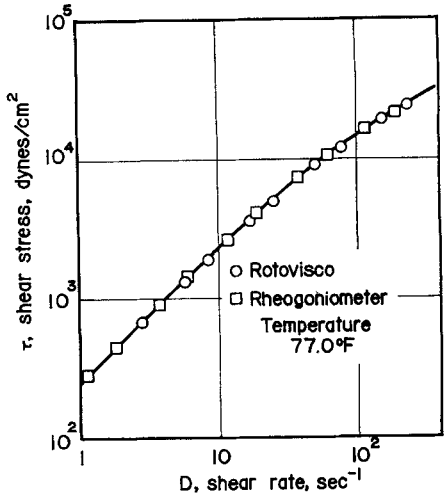

Fig. 3. Viscometric data.

STRESS AND OPTICAL RELATIONSHIPS

The two-dimensional relationships between Cartesian stress components, principal stress components, and polar stress components are obtained by straightforward coordinate transformations (5) and, after combination with Equations (11) and (12), can be summarized as

$$\tau_{xy} = \frac{\Delta\sigma}{2} \sin 2\chi_{stress} = \frac{\Delta n}{2C} \sin 2\chi_{opt} \qquad (13)$$

$$\tau_{xx} - \tau_{yy} = \Delta\sigma \cos 2\chi_{stress} = \frac{\Delta n}{C} \cos 2\chi_{opt} \qquad (14)$$

converging

$$\tau_{r\theta} = \frac{1}{2}(\tau_{yy} - \tau_{xx}) \sin 2\theta - \tau_{xy} \cos 2\theta \qquad (15)$$

$$\tau_{rr} - \tau_{\theta\theta} = (\tau_{xx} - \tau_{yy}) \cos 2\theta - 2\tau_{xy} \sin 2\theta \qquad (16)$$

diverging

$$\tau_{r\theta} = \frac{1}{2}(\tau_{yy} - \tau_{xx}) \sin 2\theta + \tau_{xy} \cos 2\theta \qquad (17)$$

$$\tau_{rr} - \tau_{\theta\theta} = (\tau_{xx} - \tau_{yy}) \cos 2\theta + 2\tau_{xy} \sin 2\theta \qquad (18)$$

Physical components of stress are understood throughout. The coordinates are sketched in Figure 1 for diverging flow. In converging flow the duct was turned end for end and the coordinates imposed so that the flow, which was from left to right, was in the positive x direction and in the negative r direction. The angle θ was defined so as to be positive in the top part of the duct in both cases. The angle χ_{opt} (or χ_{stress}) is defined to be the mathematically positive angle from the x axis to the first encountered principal optical (stress) axis. The principal difference $\Delta\sigma$ and the refractive index difference Δn are defined to be the principal value in the first quadrant minus the principal value in the second quadrant, regardless of the magnitude of the principal values. Throughout the discussion, angles will be measured from the x axis, independent of the location of the streamline. This is possible because the optical theory relates the stress directly to the birefringence, independent of the deformation mechanism which has created both effects.

Thus by measuring Δn and χ_{opt} at every point, one can calculate the shear stress and the difference in normal stresses at every point, expressed in any appropriate coordinate system. The optical angle χ_{opt} is obtained by rotating the crossed polarizer and analyzer plates together until extinction (a black line) is observed through the point under observation. That extinction will occur when the planes of polarization are coincident with the principal optical (or stress) axes is a standard result in photoelasticity and may be readily derived by considering beams of light passing along the two principal axes (*10*). By finding the optical axes, the amount of birefringence can be determined by the quarter-wave plate compensator method (Sénarmont method), described by Jessop and Harris (*10*). Physically, one measures the angular movement of the quarter-wave plate. Complete details of the optical relationships are given in the theses (*1, 28*).

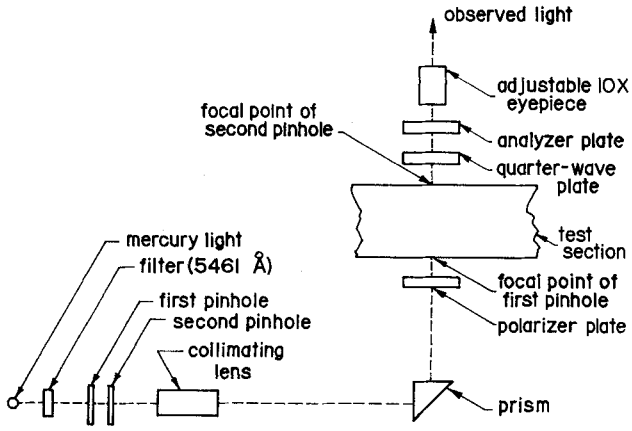

Fig. 2. Schematic diagram of optical components.

EXPERIMENTAL

Basic Equipment

The basic apparatus was designed and first operated by Whitehead, and later modified by Adams. The major components of the system will be briefly described below; complete details are available in the theses (*1, 28*).

The circulating system consists basically of a variable-speed Moyno pump, a heat exchanger, thermostating controls, a 10μ bypass filter, the test duct, and associated piping. The test duct, shown schematically in Figure 1, is constructed of Plexiglas with stress-free side walls of Vycor glass. The optical system, shown schematically in Figure 2, consists of a mercury arc lamp (Osram HB 220 w.), a filter (5,461 Å.), a double pinhole device, a prism to deflect the beam through the duct, the various Polaroid plates, and a magnifying eyepiece. The double pinhole device [suggested by Philippoff (*20*)] is arranged so that one pinhole focusses on the bottom of the duct and the other on the top; thus one is able to obtain a bright and nearly cylindrical shaft of light. The beam is about 0.032 in. in diameter in the test duct and passes through the duct in its long dimension (z direction).

The test duct is mounted on a screw mechanism for horizontal movement in the x coordinate direction. Cross channel (y direction) observation is made independent of the test duct with a traversing magnifying eyepiece and a prism-de-

flected light source. Measurements can be made in the straight ducts on either end of the converging-diverging section; distance measurements can be made to a precision of 0.001 in.

Auxiliary Equipment

Auxiliary equipment consists of a rotational Couette viscometer, a cone and plate viscometer, and a rotational polariscope to determine birefringence as a function of shear rate (*22*).

Materials

The test fluid was a 12 wt. % solution of polystyrene in Aroclor 1242. The polystyrene (Styron 666, K27-71, lot PHC93) was obtained from the Dow Chemical Company. It has a molecular weight of about 170,000, an M_w/M_d ratio of 2.0, and a density of 1.00 g./cc. The solvent was a chlorinated hydrocarbon mixture and was manufactured by the Monsanto Chemical Company. Aroclor 1242 has a density of 1.38 g./cc. and the 12 wt. % solution has a density of 1.33 g./cc.

Polystyrene in Aroclor was selected because the polymer solution is highly birefringent, nearly nonvolatile, and has been previously investigated in simple shear experiments. The 12 wt. % solution was as concentrated as could be easily used.

The solution was prepared by mixing the correct amount of of polystyrene and Aroclor (about 50 lb. total weight) in a 6½ gal. polyethylene jug and revolving the jug for about 4 wk. at 100° to 130°F. Two 500 w. heat lamps were used to heat the solution.

Runs Performed

Five runs were carried out, two in converging flow and three in diverging flow. The flow rates in the converging runs were 0.88 and 1.38 lb./min., and in the diverging runs, 0.51, 0.88, and 1.38 lb./min. The flow rates were determined by calibrating the gear box settings on the pump with a weigh tank. The temperature was controlled in the range of 77.0° to 77.5°F. Point-by-point birefringent data (Δn and χ_{opt}) were obtained in both straight channels and in the converging-diverging section in all runs. Space restrictions, however, limited the presentation of data to only the runs at a flow rate of 1.38 lb./min.

EXPERIMENTAL RESULTS

Viscometric Data

Shear stress-shear rate data, measured in the rotational viscometer (Rotovisco) and in the cone and plate viscometer (Rheogoniometer), are shown in Figure 3 and are in good agreement. For later use a power law equation

$$\tau_{12} = \text{const } D^n \tag{19}$$

was fitted to the data in the neighborhood of 20 sec.$^{-1}$ with the result $n = 0.89$.

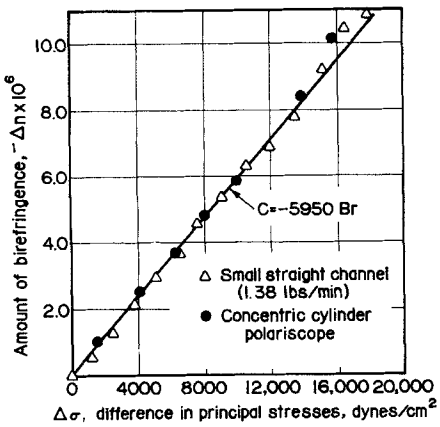

Fig. 4. Determination of the stress optical coefficient.

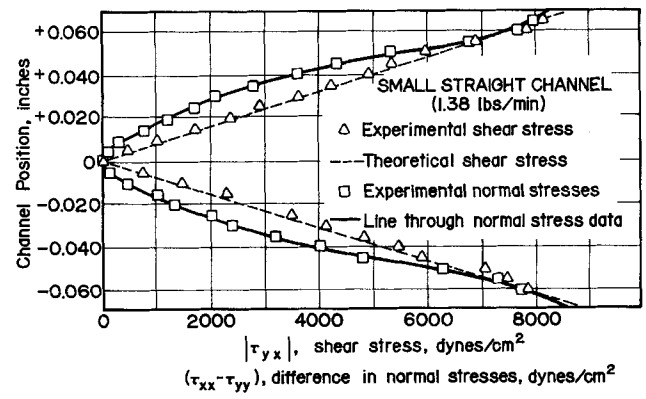

Fig. 5. Stresses in straight channel flow.

DETERMINATION OF THE STRESS OPTICAL COEFFICIENT

The stress optical coefficient C in Equation (11) can be obtained by calibration in any simple geometry in which the shear stresses are known or can be calculated. Because of initial difficulties with the Rao polariscope data (see below), the basic calibration was made in the small straight channel, with the highest flow rate data (1.38 lb./min.). This was done by calculating the shear rate at the wall from the equation for power law flow between flat parallel plates (*15*) and the linearity of shear stress in developed flow

$$|D_w| = \left(\frac{2n+1}{n}\right)\frac{2Q}{wh^2} \tag{20}$$

$$\left|\frac{\tau_{zy}(y)}{\tau_w}\right| = 2\left(\frac{y}{h}\right) \tag{21}$$

By calculation of the shear rate at the wall from Equation (10) and the use of Figure 3, the shear stress at the wall could be calculated. Equation (21) allowed one to calculate the shear stress τ_{zy} at each point. From the optical measurements Δn and χ_{opt} ($= \chi_{stress}$) were available, allowing one to calculate $\Delta\sigma$ at each point from Equation (13). Finally, Figure 4 was prepared and a stress optical coefficient of −5950 Brewsters was calculated (1 Brewster $= 10^{-13}$ sq. cm./dyne). This was in excellent agreement with a value of −5965 Brewsters obtained by Philippoff (*20*) on an actual sample used by Whitehead. Philippoff subsequently reported values of near −5820 Brewsters for various polystyrenes in Aroclor 1248 (*19*). In the concentration range studied, the birefringence was almost

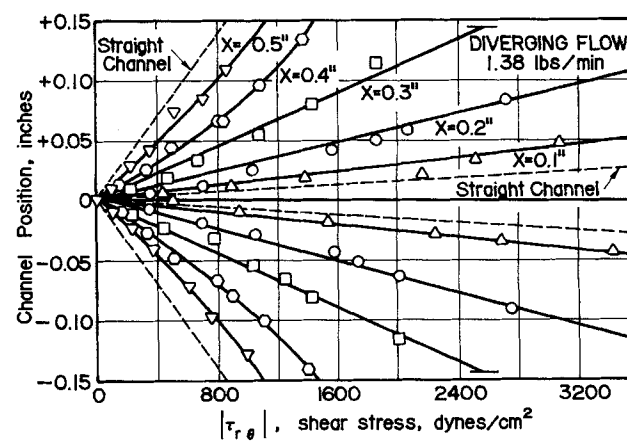

Fig. 6. Shear stresses in diverging flow.

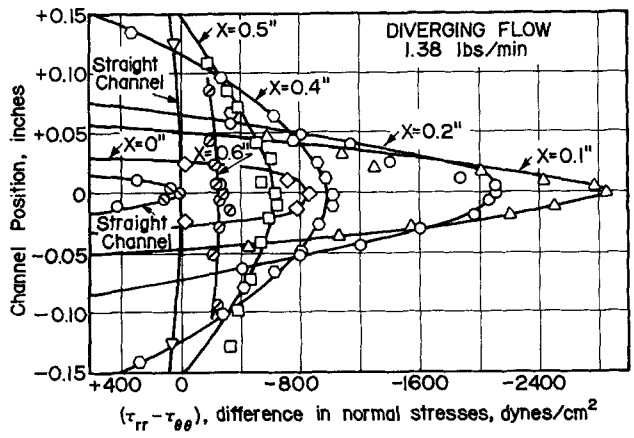

Fig. 7. Difference in normal stresses in diverging flow.

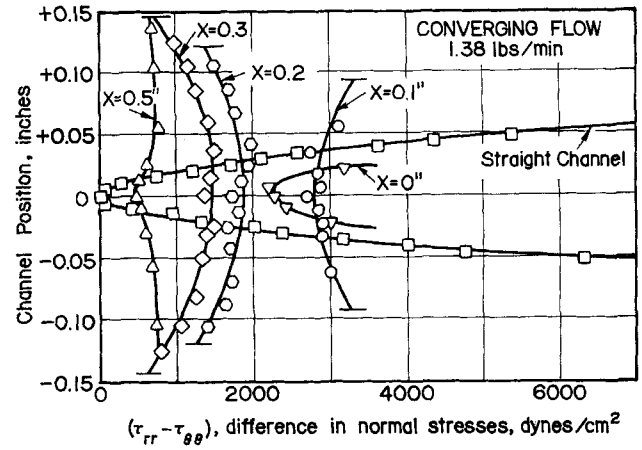

Fig. 9. Difference in normal stresses in converging flow.

entirely due to the polymer and the correction for the solvent birefringence was not needed (*19*).

A series of experiments carried out in the concentric cylinder polariscope (*1, 22*) gave stress optical coefficients consistently lower (~20%) than those reported by Philippoff. In recent months it has been established that this difficulty was due to too small a length-to-gap ratio (as low as 14); a new bob and cup set with a length-to-gap ratio of 43 was constructed and the data obtained therefrom are in good agreement with the straight channel data (Figure 4). Thus, all the data are in accord and a stress optical coefficient of −5965 Brewsters was used in the subsequent calculations.

Stresses in Straight, Converging, and Diverging Flow

Shear and normal stresses from straight channel flow are presented in Figure 5. These data come from the optical measurements through the use of Equations (13) and (14). An analysis of edge effects was also made, but these were not felt to be of major significance (*1*). The maximum error was estimated to be about 6% at the wall of the large straight channel and about 2% at the wall of the small straight channel. The estimated experimental error is of the order of 8%. Also shown, as dotted lines, are plots of Equation (21), the predicted shear stress calculated from the measured flow rate and the rheological data. (In the case of the high flow rate run, of course, the line is not entirely independent of the data, since the data were used in partial support of the stress optical coefficient calibration.) The linearity of the shear stress data and the consistent agreement is encouraging.

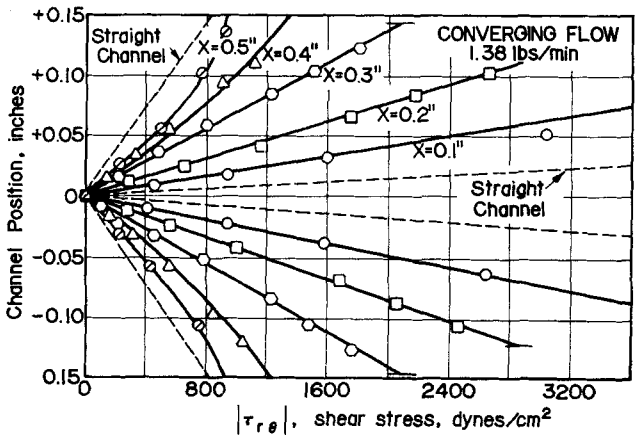

Fig. 8. Shear stresses in converging flow.

Shear and normal stress data for converging and diverging flow are presented in Figures 6, 7, 8, and 9. The traverses across the channel were in straight lines and are identified by the distance parameter X, as shown in Figure 1. The appearance of normal stresses throughout is not surprising, since the flow is an accelerative one and some normal stresses would be expected even in Newtonian flow.

ANALYSIS IN TERMS OF THE SECOND-ORDER COLEMAN-NOLL THEORY

The simplest constitutive equation which predicts normal stress, although not non-Newtonian viscosities, is the second-order theory of Coleman and Noll (*7*), given by

$$\tau_{ij} = -pg_{ij} + \eta d_{ij} + \beta d_i{}^k\, d_{kj} + \gamma A_{ij}^{(2)} \qquad (22)$$

where $d_{ij} = v_i|_j + v_j|_i$, deformation rate tensor

$$A_{ij}^{(2)} = \frac{\partial\, d_{ij}}{\partial t} + v^k\, d_{ij}|_k + d_{ik}\, v^k|_j + d_{kj}\, v^k|_i$$

second Rivlin-Ericksen tensor, η, β, γ = material constants. In straight line shearing flow, with D as the shear rate, this theory yields the following results:

$$\tau_{xy} = \eta D \qquad (23)$$

and

$$\tau_{xx} - \tau_{yy} = -2\gamma D^2 \qquad (24)$$

Because of the low shear rates in the present work the viscosity is relatively constant (see Figure 3) and thus Equation (23) is approximately correct. More interesting is Equation (24), which predicts a dependence of the normal stresses on the square of the shear rate. The straight channel data are so plotted in Figure 10 and compared with data from the concentric cylinder polariscope. A constant γ in Equation (24) would provide a reasonable approximation to the data. The deviation of the channel data at higher shear rates is typical of polymer systems (*6*), although this may well be an optical problem due to reflections near the wall of the channel. Constants of η = 210 dyne (sec.)/sq. cm. and γ = − 3.2 dyne (sec.^{2})/sq. cm. were fitted to the data for later use.

Converging and diverging flow in channels can be rigorously treated for Newtonian fluids by the use of the following substitution (*12*):

$$v_r = f(\theta), \text{ a function of } \theta \text{ only} \qquad (25)$$

Physically one is assuming flow along rays, with no velocity in the θ direction. This substitution is rigorously

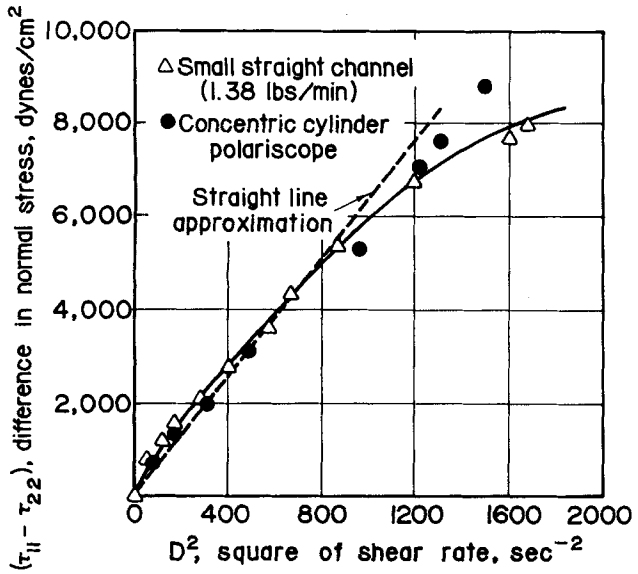

Fig. 10. Difference in normal stresses vs. square of the shear rate.

correct in Newtonian flow in that it satisfies identically the continuity equation and the equations of motion. For viscoelastic fluids it is a reasonable first approximation for an iterative treatment (*12*). Writing out Equation (22) in polar, (r, θ), coordinates and inserting Equation (25), one finally obtains the results

$$\tau_{r\theta} = \eta \frac{f'}{r^2} - 4\gamma \frac{f'f}{r^4} \tag{26}$$

and

$$\tau_{rr} - \tau_{\theta\theta} = -4\eta \frac{f}{r^2} + \frac{\gamma}{r^4}[8f^2 - 2f'^2] \tag{27}$$

Physical components of stress are understood throughout. For flow of a Newtonian fluid at low Reynolds number in channels of modest angles, the rigorous Jeffery-Hamel velocity profile solution approaches a parabolic distribution (*16*). Using this information one has

$$f = -\frac{3Q}{4w\alpha}\left[1 - \left(\frac{\theta}{\alpha}\right)^2\right] \quad \text{(converging)} \tag{28}$$

and

$$f = +\frac{3Q}{4w\alpha}\left[1 - \left(\frac{\theta}{\alpha}\right)^2\right] \quad \text{(diverging)} \tag{29}$$

Inserting Equations (28) and (29) into Equations (26) and (27), one obtains

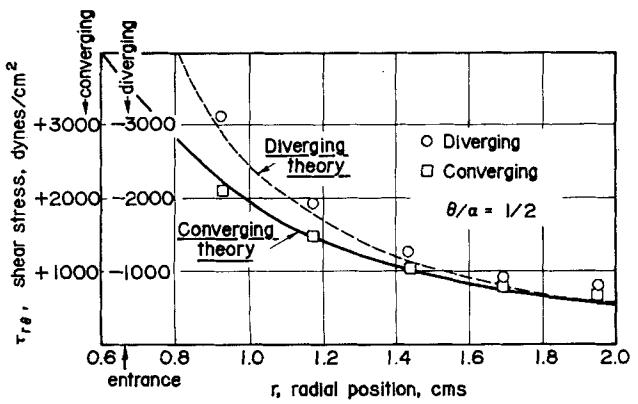

Fig. 11. Comparison of experimental shear stresses with theory.

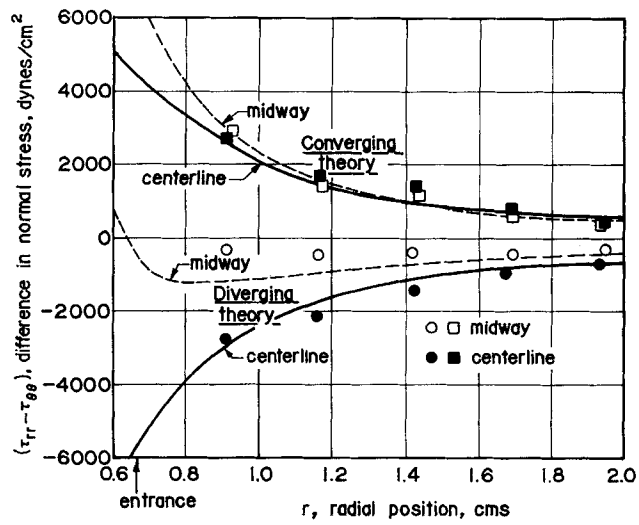

Fig. 12. Comparison of experimental normal stresses with theory.

$$\tau_{r\theta} = \pm\frac{3}{2}\eta\left(\frac{Q}{w\alpha}\right)\left(\frac{\theta}{\alpha}\right)\frac{1}{r^2\alpha} - \frac{9(-\gamma)}{2r^4\alpha}\left(\frac{Q}{w\alpha}\right)^2\left(\frac{\theta}{\alpha}\right)\left[1-\left(\frac{\theta}{\alpha}\right)^2\right] \tag{30}$$

and

$$\tau_{rr} - \tau_{\theta\theta} = \pm\frac{3\eta}{r^2}\left(\frac{Q}{w\alpha}\right)\left[1-\left(\frac{\theta}{\alpha}\right)^2\right] - \frac{9}{2}\frac{(-\gamma)}{r^4}\left(\frac{Q}{w\alpha}\right)^2\left\{\left[1-\left(\frac{\theta}{\alpha}\right)^2\right]^2 - \left(\frac{\theta}{\alpha}\right)^2\frac{1}{\alpha^2}\right\} \tag{31}$$

The top sign is for converging flow, the bottom sign for diverging flow. By making these approximations one is able to obtain explicit results and thus note the contributions of the various terms to the predicted stresses.

Equations (30) and (31) have been plotted as the theory lines in Figures 11 and 12, using the material constants η and γ previously determined. Two angular positions were selected: the centerline $(\theta/\alpha = 0)$ and the midway line $(\theta/\alpha = \frac{1}{2})$. Considering that there are no adjustable parameters in these equations, the agreement is remarkably good. It is most encouraging that the difference between the two curves in Figure 11, which is due to the γ term, accurately reflects the data. Also the normal stress lines at $\theta/\alpha = \frac{1}{2}$ are influenced significantly by both the η term and the γ term, again bearing out the generally correct character of the γ term in fitting the data. The data at $X = 0$, exactly at the entrance (or exit), do not seem to bear any relation to the developed flow curves shown and are not plotted. These data, however, may be of considerable interest in a rigorous analysis because of the distorted flow patterns near the vertex (*12*).

FUTURE WORK AND CONCLUDING REMARKS

The theoretical analysis presented here is a preliminary one, intended to show that the general features of the stress data are in agreement with accepted theory. It is planned to pursue this type of analysis in more detail and to consider other constitutive equations, in particular, higher-order empirical modifications of the Coleman-Noll theory (*4, 27*), and the elastic fluid theory of Bernstein, Kearsley, and Zapas (*2*). Some of the modifications of the Oldroyd three-constant model suggested by Bird and coworkers (*3*) might be applicable, although the appearance of a stress derivative with respect to time in these equations makes analysis of accelerative flows difficult.

Experimentally, photographic velocity profile studies are in progress, to be followed by studies of the 90-deg. or sharp entrance problem. As part of the velocity studies, special attention will be devoted to trying to detect the secondary or spiralling flows, characteristic of viscoelastic flow in noncircular ducts (*12*). It is not felt, however, that this will be an important effect, judging from visual observations made thus far.

In summary, it is concluded that the birefringent method can be used for measuring stresses in viscoelastic, accelerative flows and that the Coleman-Noll second-order theory accurately correlates such data at low shear rates.

ACKNOWLEDGMENT

This project has been almost entirely supported by the National Science Foundation under Grants G-22091 and GP-2732. A portion of the related theoretical work was carried out while one of the authors (EBA) was being supported by a grant from the National Aeronautics and Space Administration (NsG 671). The help of these organizations is greatly appreciated. Also the authors particularly wish to thank Dr. W. Philippoff for carrying out birefringent measurements on several of our samples and for his helpful comments on many different occasions.

NOTATION

$A^{(2)}_{ij}$ = second Rivlin-Ericksen tensor, see Equation (22)
C = stress optical coefficient, defined by Equation (11), sq. cm./dyne
c = speed of light in vacuum, cm./sec.
D = shear rate, sec.$^{-1}$
$\mathbf{D}_i$ = electric displacement vector
d_{ij} = deformation rate tensor, see Equation (22)
$\mathbf{E}_i$ = electric field vector
$f(\theta)$ = v_r, a new velocity variable, sq. cm./sec.
g_{ij} = metric tensor
h = height of channel, cm.
K_0 = permittivity of a vacuum
n = power law constant, dimensionless
n_1, n_{11} = principal refractive indices
p = arbitrary scalar stress, dyne/sq. cm.
$\mathbf{P}_i$ = polarization vector
Q = volumetric flow rate, cc./sec.
r = radial position, cm.
v_1, v_{11} = velocity of light along the principal axes, cm./sec.
$v_{i|j}$ = covariant derivative of velocity
v_r = physical component of velocity in r direction, cm./sec.
$X^i{}_j$ = dielectric susceptibility tensor
w = depth of channel, cm.
x,y,z = Cartesian coordinates, cm.

Greek Letters

α = half angle of duct
β = material constant, (dyne)(sec.^{2})/sq. cm.
γ = material constant, (dyne)(sec.^{2})/sq. cm.
Δn = $n_I - n_{II}$, difference in principal refractive indices
$\Delta\sigma$ = $\sigma_1 - \sigma_{II}$, difference in principal stresses
ϵ = arbitrary scalar susceptibility, dimensionless
η = material constant, the viscosity (dyne)(sec.)/sq. cm.
θ = angular coordinate
λ_1, λ_{II} = principal extension ratios
ξ = material constant, sec.
τ_{ij} = tensor components of stress
$\tau_{12}, \tau_{11}, \tau_{22}$ = physical components of stress in general (1 = direction of flow), dyne/sq. cm.
$\tau_{xy}, \tau_{xx}, \tau_{yy}$ = physical components of stress in Cartesian coordinates, dyne/sq. cm.
$\tau_{r\theta}, \tau_{rr}, \tau_{\theta\theta}$ = physical components of stress in polar coordinates, dyne/sq. cm.
χ_{opt} = optical angle, angle between x axis and first principal axis of susceptibility tensor
χ_{stress} = principal stress angle, angle between x axis and first principal stress axis

Subscripts

w = quantity evaluated at the wall
I,II,III = principal values

LITERATURE CITED

1. Adams, E. B., M.S. thesis, Univ. Tennessee, Knoxville (December, 1964).
2. Bernstein, Barry, E. A. Kearsley, and L. J. Zapas, *Trans. Soc. Rheol.*, **7**, 391-410 (1963); also L. J. Zapas, paper presented at the Soc. Rheol. Pittsburgh meeting (October, 1964).
3. Bird, R. B., paper presented at A.I.Ch.E. Boston meeting (December, 1964).
4. Bogue, D. C., *NSF GP-2005 Rept. No. 1*, Univ. Tennessee, Knoxville (August, 1964).
5. Bogue, D. C., and F. N. Peebles, *Trans. Soc. Rheol.*, **6**, 317-23 (1962).
6. Brodnyan, J. G., F. H. Gaskins, and Wladimir Philippoff, *Trans. Soc. Rheol.*, **1**, (1957).
7. Coleman, B. D., and Walter Noll, *Arch. Rat. Mech. Anal.*, **6**, 355-70 (1960).
8. Coleman, B. D., and R. A. Toupin, "Notes Toward a Theory of Dielectrics with Memory," Mellon Inst., Pittsburgh (circa 1962).
9. Ginn, G. F., and A. B. Metzner, in "Proc. 4th Intern. Congr. Rheol.," pp. 583-601, Interscience, New York (1963).
10. Jessop, H. T., and F. C. Harris, "Photoelasticity: Principles and Methods," Cleaver-Hume Press Ltd., London (1949), Dover reprint S720.
11. Kuhn, W., and F. Grün, *Kolloid Z.*, **101**, 248 (1942).
12. Langlois, W. E., and R. S. Rivlin, *Tech. Rept. No. 3, Contract DA-19-020-ORD-4725, Army Ord. R & D.*, Brown Univ., Providence (December, 1959); published in part in W. E. Langlois, *Trans. Soc. Rheol.*, **7**, 75-99 (1963).
13. Lodge, A. S., *Kolloid Z.*, **171**, 46-51 (1960).
14. Markovitz, Hershel, and D. R. Brown, *Trans. Soc. Rheol.*, **7**, 137 (1963).
15. McKelvey, J. M., "Polymer Processing," Wiley, New York (1962).
16. Millsaps, Knox, and Karl Pohlhausen, *J. Aeronaut. Sci.*, **20**, 187-196 (1953).
17. Nye, J. F., "Physical Properties of Crystals," Appendix H, Oxford Press, London (1957).
18. Philippoff, Wladimir, *Trans. Soc. Rheol.*, **1**, 95-107 (1958); **4**, 159-168, 169-177 (1960); **7**, 45-59 (1963).
19. ———, paper presented at 4th Intern. Congr. Rheol., Providence (August, 1963).
20. ———, private communication.
21. Prados, J. W., and F. N. Peebles, *A.I.Ch.E. J.*, **5**, 225-234 (1959).
22. Rao, S. S., M.S. thesis, Univ. Tennessee, Knoxville (October, 1963).
23. Read, B. E., *Polymer*, **3**, 143-52 (1962).
24. ———, "Techniques of Polymer Science," SCI Monograph No. 17, p. 198, Soc. Chem. Ind., London (1963).
25. Stein, R. S., S. Onogi, and D. A. Keedy, *J. Polymer Sci.*, **57**, 801-821 (1962); quoting R. S. Stein and A. V. Tobolsky, *Textile Res. J.*, **18**, 302 (1948).
26. Treloar, L. R. G., *Trans. Faraday Soc.*, **4**, 277 (1947); also "Physics of Rubber Elasticity," 2 ed., Oxford Press, London (1958).
27. White, J. L., and A. B. Metzner, *A.I.Ch.E. J.*, **11**, 324-330 (1965).
28. Whitehead, J. C., M.S. thesis, Univ. Tennessee, Knoxville (January, 1964).
29. Yamada, R., C. Hayashi, S. Onogi, and M. Horio, *J. Polymer Sci.*, Pt. C; "Polymer Symposia No. 5: Rheo-Optics of Polymers," Interscience, New York (1964).

Manuscript submitted February 16, 1965; revision received July 10, 1965; paper accepted July 26, 1965. Paper presented at A.I.Ch.E. Philadelphia meeting.